ELSEVIER

Biochimica et Biophysica Acta 1564 (2002) 487–499

BIOCHIMICA ET BIOPHYSICA ACTA
BBA

www.bba-direct.com

Cadmium transport through type II alveolar cell monolayers: contribution of transcellular and paracellular pathways in the rat ATII and the human A549 cells

C. Jumarie *

Département des Sciences Biologiques, Toxen, Université du Québec à Montréal, C.P. 8888, Succ. centre-ville, Montréal, Québec, Canada H3C 3P8

Received 18 January 2002; received in revised form 18 June 2002; accepted 27 June 2002

Abstract

Cadmium (Cd) transport in alveolar type II (ATII) cells has been studied using two in vitro models widely used to investigate lung function: primary cultures of rat ATII cells and the human cell line A549. Nonlinear regression analyses of the uptake time-course of ^{109}Cd revealed: a zero-time accumulation, a fast process of accumulation which proceeds within minutes, and a much slower process which takes hours. This three-step mechanism was characterized by different parameter values under dishes-or filter-growth conditions. A higher initial uptake rate (v_i) and equilibrium accumulation (A_{max}) of ^{109}Cd were found in the rat ATII cells; these differences were not related to a higher level of adsorption onto the external surface of the cell membrane. Specific transport systems of similar capacity but different affinity (threefold higher in rat cells) were characterized. A significant transepithelial transport of ^{109}Cd, with similar P_{coeff} in both cell models, could not be exclusively related to cellular metal release. Results on ^{3}H-mannitol permeability together with ^{109}Cd efflux data strongly suggest a greater contribution of the paracellular pathways in Cd transport through A549 cell monolayers. These differences in transport properties between the two lung cell models may modify the dose–response curve for Cd toxicity.

Keywords: Cadmium; Metal transport; Epithelium permeability; Paracellular barrier; Type II cell; A549 cell

1. Introduction

Relevant human exposure to cadmium (Cd) occurs via the ingestion of food and drinking water and through the inhalation of contaminated air. Though the main exposure to Cd for nonsmoking people under normal conditions is oral intake, uptake by inhalation may increase significantly especially in specific workplaces where atmospheric Cd levels have been shown to be rather high; Cd uptake by inhalation can exceed that from ingestion in some industrial and residential polluted areas. It is well known that this metal is partially accumulated in the lung, and lung toxicity includes acute inflammatory effects, chronic edema and bronchitis, as well as cancer [1–4]. As for most toxic substances, one determinant in Cd toxicity is its availability for the lung as well as its bioavailability through inhalation (that fraction of the inhaled metal that crosses the alveolar epithelium and that is available for tissue distribution via blood circulation). Cadmium absorption and lung deposition vary with the inhaled particle size; it has been shown that particle deposition in the alveoli remains significant for diameters smaller than 2–3 μm, whereas particles of larger diameters deposit preferentially in the naso-pharyngial region of the respiratory tract [5]. Also, it is now well recognized that bioavailability of the inhaled metal, as well as Cd toxicity, vary considerably with the chemical species of concern, namely Cd speciation. Cadmium chloride, sulfide and oxide are the most relevant metal compounds for human exposure, particularly the two latter for occupational exposure. However, both Cd oxide and sulfide are rather insoluble in water and Cd sulfide bioavailability has been suggested as being very low [6].

The lung epithelium represents the first barrier to be crossed by the inhaled metal but also the first target organ following metal inhalation. The adult pulmonary epithelium is composed of two cell types that are specialized for distinct functions. Type I cells, which represent about 95% of the alveolar surface, are spread cells, whereas type II cells are polarized and develop microvilli at their apical domain faced to the alveoli with tight junctions between them. Type II cells are responsible for surfactant synthesis and storage in lamel-

* Tel.: +1-514-987-3000x7680; fax: +1-514-987-4647.
E-mail address: jumarie.catherine@uqam.ca (C. Jumarie).

0005-2736/02/$ - see front matter © 2002 Elsevier Science B.V. All rights reserved.
PII: S0005-2736(02)00499-6

lar bodies, express numerous polarized transport systems, and have been shown to have an important role in pulmonary fluid clearance [7,8]. Most of the cyt. *P*450 activity of the lung has been attributed to this cell type [9]. It is also known that following lung injury with significant type I cell necrosis, type II cells proliferate and, by undergoing a "de-differentiation" or a "trans-differentiation" process, cover the injured alveolar surface [10]. Controversy still exists on whether or not type II cells represent the stem cells for type I cells, but it is well known that cell types are present at a constant ratio [11].

In an attempt to better understand pulmonary Cd cytotoxicity, studies investigating parameters that may modulate cell sensitivity have been conducted in primary cultures of rat type II cells as well as in the human lung carcinoma cell line A549, which has been shown to express numerous features of the normal type II cells including surfactant synthesis [12,13], expression of cyt. *P*450 isozymes [14], cation transporters and amiloride-sensitive Na^+ channels [15,16], as well as choline transport mechanisms [17]. Most of these studies have focused on the role of intracellular protective compounds such as metallothionein (MT) and reduced glutathione (GSH) [18–20] but few have been devoted to the mechanisms of transport into and across the alveolar cells. Moreover, rat alveolar type II (ATII) and A549 cells represent two in vitro models widely used to investigate alveolar cell function but we do not know to what extent the results for Cd obtained in the cell line compared with data in rat cells. We have therefore characterized Cd uptake in A549 cells as well as in primary cultures of type II cells isolated from rat. The main goals of our study were: (i) to compare kinetic parameter values for Cd uptake in the two alveolar cell models, and (ii) to evaluate the respective contribution of paracellular and transcellular pathways in the transepithelial transport of Cd through ATII cell monolayers. These points are critical determinants of the pulmonary absorption and lung toxicity of the inhaled metal. Our results point out similarities and differences between the two cell models: higher initial uptake rate (v_i) and equilibrium accumulation (A_{max}), higher affinity (lower K_m value) as well as a higher contribution of the transcellular pathways to Cd transport through cell monolayers in rat ATII cells compared to the human A549 cell line. They also show that although cell monolayers form barriers relatively resistant to mannitol, paracellular pathways may contribute to significant transepithelial transport of Cd.

2. Materials and methods

2.1. Cell culture

2.1.1. Cell line A549

Cell line A549, obtained from the American Type Culture Collection, was maintained in Ham's F12 medium (50 units/ml penicillin, 50 μg/ml streptomycin) supplemented with 10% heat-inactivated fetal bovine serum (FBS) and 1 mM glutamine. Cells were routinely grown in 75-cm^2 culture flasks at 37 °C in a 5% CO_2–95% humidified air atmosphere and were passaged weekly by trypsinization (0.05% trypsin–0.053 mM EDTA). For all the experiments, cells were seeded at 12.5×10^3 cells/cm^2 in 35-mm diameter petri dishes (Falcon) or in tissue-treated polyester membranes (Costar Transwell-Clear cell culture inserts), 24-mm diameter, 0.4-μm pore size. Cell cultures were maintained for 14 days (most of studies showing that A549 cells express an ATII-like phenotype were carried out on post-confluent cultures) and the culture medium was changed every 2 days. Cells were used between passages 79 to 85.

2.1.2. Primary culture of rat ATII cells

ATII cells were isolated from male Sprague–Dawley rats according to the method of Dobbs et al. [21]. Briefly, perfused lung was digested with elastase and the ATII cells were purified by differential adherence on bacteriological plastic dishes coated with rat IgG. The cells were maintained in MEM medium (0.2% $NaHCO_3$, 0.01 M HEPES, 80 μg/l gentamicin) supplemented with 10% FBS and 2 mM glutamine. Cells were seeded at 2×10^5 cells/cm^2 in 24-mm-diameter six-well plates (Falcon) and were maintained only for 3 days at 37 °C in a 5% CO_2–95% humidified air atmosphere to avoid the well known transdifferentiation to the ATI phenotype occurring by day 4 or 5 [22–24].

2.2. Accumulation and transport measurements

Cellular Cd accumulation and transcellular transport experiments were performed at room temperature on 14-day-old A549 and 3-day-old type II cell monolayers, grown on petri dishes or microporous membranes in a defined transport medium containing (in mM): 137 NaCl, 5.9 KCl, 1.2 $MgSO_4$, 2.5 $CaCl_2$, 4 D-glucose and 10 HEPES, adjusted to pH 7.3 by addition of 5 mM NaOH. The monolayers were washed four times with 2 ml (Petri dishes or AP side) and 3 ml (BL side) of ^{109}Cd-free transport medium in order to remove the serum-containing culture medium. Accumulation was started by incubating the cells in 2 ml (petri dishes or AP exposure) transport medium containing 0.3 μM of ^{109}Cd-labeled $CdCl_2$ (sp. act. from 0.24 to 0.33 mCi/μmol). In some cases, experiments were carried out in the presence of various concentrations of unlabeled Cd used as a pure competitive inhibitor [25,26]; in all cases, values of accumulation are reported relative to tracer ^{109}Cd exclusively. Mannitol transport experiments were performed as in Cd transport measurements using an exposure medium containing 0.3 μM of ^{3}H-labeled mannitol (sp. act. 19.03 Ci/mmol).

Tracer accumulation was stopped by removing the transport medium, and the monolayers were rapidly rinsed four times with 2 ml (petri dishes or AP side) and 3 ml (BL side) of ice-cold ^{109}Cd-free (or ^{3}H-mannitol-free) transport medium in order to remove the excess radioactivity. In some experiments, these rinses were performed with 2 mM EDTA-containing stop solution (Ca^{2+}-, Mg^{2+}-free)

to extract the external labile metal fraction from the cell surface. Cells from dishes were then solubilized in 1 N NaOH (0.5 ml) and aliquots of 0.3 ml were used for radioactivity determination using a gamma counter (Cobra II, Canberra Packard Canada), while 50 μl of the remaining suspension was kept for protein assay. For experiments performed on cells grown on microporous membranes, 1 ml of the BL medium was retained before the filters were carefully cut off from the inserts. Cells and media samples were then used for radioactivity determination. Cells from three monolayers of the same subculture were washed with PBS, harvested and pooled together for protein determination. In the present paper, accumulation refers to the total amount of ^{109}Cd measured in cell samples (adsorption + uptake), uptake data correspond to the metal that actually crosses the cell membrane (accumulation− adsorption), whereas adsorption refers to the metal bound to the cell surface (accumulation—uptake), namely the EDTA-sensitive labile component of accumulation. On the other hand, transport data (transepithelial transport) refer to the total amount of ^{109}Cd tracer (or ^{3}H-mannitol) that crosses the monolayers and that is recovered in the BL medium following AP exposure. Both accumulation and transport are expressed as pmol ^{109}Cd (or ^{3}H-mannitol) per mg protein, the amount of tracer transported being calculated for the total volume (3 ml) of the medium in the BL compartment.

2.3. Cadmium efflux measurements

Cadmium efflux measurements were performed at room temperature on 14-day-old A549 and 3-day-old type II cell monolayers grown on microporous membranes. The cells were first exposed on the AP side to 0.3 μM ^{109}Cd for 1 h, at which time accumulation processes were stopped as described in the previous section, but using room-temperature stop solution. The cells were then incubated in 2-ml (dishes and AP compartment) or 3-ml (BL compartment) ^{109}Cd-free medium. At specific times of efflux, 1 ml of both the AP and the BL media were sampled and the cells were washed rapidly with ice-cold stop solution. The filters were then excised from the inserts, and samples of the cells and the media were used for radioactivity determinations. EDTA-containing solutions were not used as the efflux medium since the lack of Ca^{2+} in such media might be expected to disrupt the intercellular tight junctions, leading to artifactual paracellular leakage.

2.4. Data analyses

2.4.1. Accumulation studies

Nonlinear regression analyses of the accumulation (A) time-course data obtained over a 12-h exposure were performed using first-order rate Eq. (1)

$$A = A_{e(f)}(1 - e^{-k_{A(f)}t}) + A_{e(s)}(1 - e^{-k_{A(s)}t}) + A_0 \quad (1)$$

in which A_0 represents the zero-time accumulation value, $A_{e(f)}$ and $A_{e(s)}$ stand for the equilibrium accumulation values achieved with rate constants $k_{A(f)}$ and $k_{A(s)}$, respectively.

Accumulation (and uptake) data obtained under initial rate (zero-trans) conditions were analysed according to linear Eq. (2)

$$A = vt + A_0 \quad (2)$$

in which the initial rate v of accumulation (uptake) is the slope of the regression line.

2.4.2. Efflux studies

Nonlinear regression analyses of the efflux (E) time-course data were performed using first-order decay Eq. (3)

$$E = (E_0 - E_e)e^{-k_E t} + E_e \quad (3)$$

in which E_0 represents the cellular accumulation of ^{109}Cd at time $t = 0$ of efflux, and E_e stands for the plateau of efflux reached with the first order rate constant k_E. Data obtained for the cellular ^{109}Cd released (R) in the AP or the BL compartment were analysed according to first-order rate Eq. (4)

$$R = R_e(1 - e^{-k_R t}) \quad (4)$$

in which R_e stands for the maximal amount of Cd that it is recovered in the efflux medium with the rate constant k_R.

For all time-course studies, the $t_{1/2}$ values reported in this paper represent the time for which processes are half-completed. Their numerical values were calculated using Eq. (5)

$$t_{1/2} = \frac{\ln 2}{k} \quad (5)$$

in which k represents any of the rate constants estimated in Eqs. (1)–(4).

2.4.3. Kinetic parameter determinations

Kinetic data of ^{109}Cd accumulation obtained by one-time point measurements at 1 min were analyzed using the modified Michaelis–Menten Eq. (6)

$$v = \frac{V_{max} T}{K_m + T + S} + k_D T \quad (6)$$

in which K_m and V_{max} have their usual meaning, and T and S stand for tracer (0.3 μM) and unlabeled Cd concentrations (0–1000 μM), respectively. As previously discussed, k_D, which represents all nonspecific contributions to the uptake, is considered as an operational parameter only [25].

2.4.4. Permeability coefficient determinations

The apparent permeability coefficients for ^{109}Cd and ^{3}H-mannitol were determined according to Eq. (7)

$$P_{coeff} = \frac{dQ}{dt}\frac{1}{AC_{AP}} \quad (7)$$

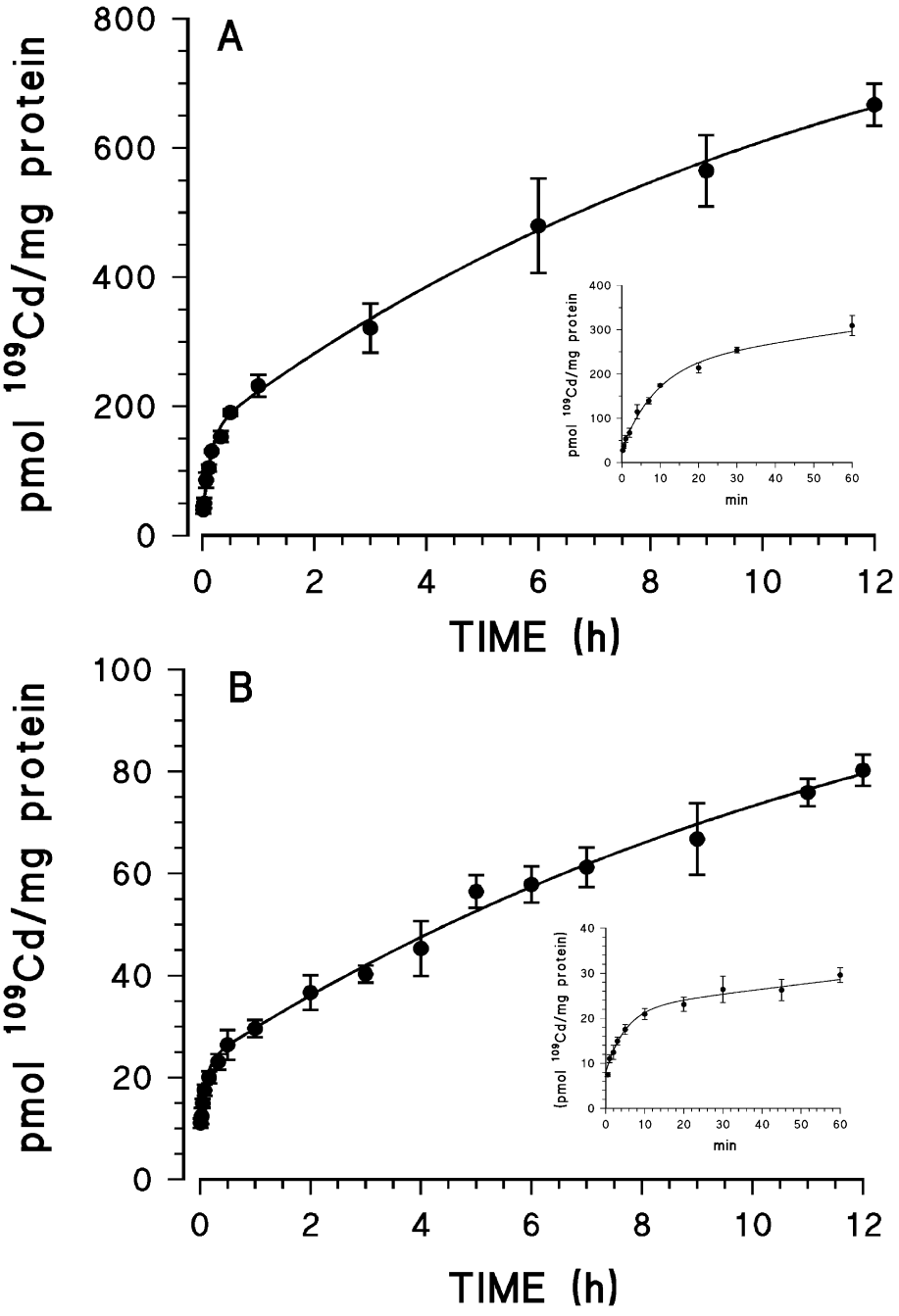

Fig. 1. Time-course of 0.3 μM ^{109}Cd accumulation in 3-day-old rat ATII cells (A) and 14-day-old A549 cells (B) grown on petri dishes. Accumulation measurements were performed as described in the text. Points shown are means ± S.D. evaluated on three different cell cultures. The lines shown are the best-fit curves over the data points as obtained according to the first-order rate Eq. (1). The uptake parameters are listed in Table 1. Insets: 1-h time-course of tracer accumulation.

where dQ/dt is the steady state flux (mol/s), C_{AP} is the initial apical concentration (mol/ml), and A is the surface area of the membrane (4.52 cm^2).

All nonlinear regression analyses of the uptake, efflux and kinetics data, as well as linear regression analyses of the uptake data obtained in short-time experiments, were performed using Enzfitter (Robin J. Leatherbarrow, Copyright © 1987) and Prims3 (GraphPad software, Inc, Copyright © 2001) software. The errors associated with the kinetic parameter values given in the text represent the standard errors of regression (SER).

2.5. Materials

All culture ware (Falcon) was obtained from VWR Scientific (Toronto, Ont.). Minimal essential and Ham's F-12 media, penicillin, gentamicin, streptomycin and trypsin were purchased from Gibco BRL (Grand Island, NY), whereas

FBS was obtained from Medicorp Inc. (Montréal, QC). Glutamine and Rat Ig-G were obtained from Sigma Chemical Co. (St. Louis, MO), whereas elastase was purchased from Worthington (Lakewood, NJ). Labeled $^{109}CdCl_2$ and ^{3}H-mannitol were obtained from Dupont Canada Inc. (Mississauga, ON), and unlabeled $CdCl_2$ from Sigma. All salts and chemicals used for buffer preparation were ACS reagents or of higher purity.

3. Results

3.1. Kinetic characteristics of Cd uptake

The time-courses of 0.3 μM ^{109}Cd accumulation in the rat ATII (Fig. 1A) and the A549 cells (Fig. 1B) grown on petri dishes could both be well analyzed according to the first-order rate Eq. (1) which describes a zero-time (A_0), a fast (A_f) and a slow (A_s) process of accumulation, the latter being responsible for most of the maximal cellular accumulation (insets allow a better view of the 1-h time-courses). It clearly appears that the rat ATII cells accumulate much higher levels of ^{109}Cd compared to the A459 cells, with the following differences: (i) a 2.5-fold higher A_0 value; and (ii) a near 10-fold higher equilibrium accumulation is obtained for both the fast and the slow processes ($A_{e(f)}$ and $A_{e(s)}$ in Table 1). Interestingly, no significant differences could be observed between the $t_{1/2}$ values, showing that similar periods of time are needed for each process of accumulation to be completed in both cell samples.

The observed differences between equilibrium accumulation values may be underestimated. Indeed, considering an average cell density of 0.4 ± 0.05 and 0.9 ± 0.1 mg/dish for the ATII and the A549 cells, respectively, the mean accumulation values of 666 ± 23 and 80 ± 3 pmol/mg protein obtained following a 12-h exposure represent a cellular ^{109}Cd content of 266 ± 16 and 72 ± 12 pmol per petri dish, which is about 44% and 12% of the total tracer initially present in the uptake medium (600 pmol/2 ml). These estimates compared quite well with direct measurements of ^{109}Cd concentration in the transport medium following a 12-h exposure of the cell samples. Indeed, decreases of 39% (0.183 vs. 0.300 μM) and 16% (0.253 vs. 0.300 μM) in tracer levels were recorded for the ATII and the A549 cells, respectively. Rapid tracer depletion from the uptake medium may contribute, in part, to the leveling off in ^{109}Cd accumulation; thus the $A_{e(f)}$ and $A_{e(s)}$ values may be underestimated, especially for the rat ATII cells. Nevertheless, from a qualitative point of view, accumulation parameter values reported in Table 1 clearly reveal that ^{109}Cd accumulates much more in the rat type II cells than in the cell line.

Table 2
Tracer levels measured in rat alveolar type II cells grown on petri dishes following exposure to 0.3 μM ^{109}Cd for different times with respect to different washing solutions

Time	Std (pmol/mg protein)	EDTA (pmol/mg protein)	EDTA-sensitive (%)
15 min	116 ± 10	94 ± 6	18.9
30 min	136 ± 12	123 ± 7	9.6
1 h	187 ± 18	165 ± 15	11.7
3 h	308 ± 15	279 ± 13	9.4
6 h	407 ± 16	398 ± 18	2.2
9 h	535 ± 17	519 ± 11	2.9
12 h	581 ± 24	569 ± 30	2.1

Following exposure for the desired time, cells were rapidly rinsed in the absence (Std) or in the presence (EDTA) of 2 mM EDTA added in the cold stop solution. Consequently, the relative percentage of EDTA-sensitive labile fraction of ^{109}Cd accumulation has been calculated as explained in the text.

In order to discriminate between uptake into the cells and adsorption onto the cell surface, cellular ^{109}Cd levels were also measured in cell samples washed with a 2 mM EDTA-containing stop solution. For a 15-min exposure, the adsorption contribution to the total metal accumulation was 19% and 7% in rat ATII (Table 2) and A549 (Table 3) cells, respectively; this contribution of adsorption decreased rapidly for longer periods of exposure. Note that even for short exposure times, the differences observed between accumulation (obtained with standard rinses) and uptake data (obtained with EDTA rinses) were not statistically significant. Consequently, the higher accumulation values obtained in the rat type II cells cannot be related to higher levels of adsorption.

3.2. Initial uptake rate of specific and nonspecific transport of Cd

The initial rate (v) of tracer accumulation/uptake has been compared in both cell models following very short exposure times. Because ^{109}Cd accumulation could be approximated by straight lines only up to 4- and 2-min incubation for the rat and the A549 cells, respectively (data not shown), the initial rate of tracer accumulation/uptake was estimated over

Table 1
Parameter values describing the time-course of ^{109}Cd accumulation aver a 12-h exposure in primary culture of rat alveolar type II cells and in the A549 cells

	A_0 (pmol/mg protein)	$A_{e(f)}$ (pmol/mg protein)	$t_{1/2(f)}$ (min)	$A_{e(s)}$ (pmol/mg protein)	$t_{1/2(s)}$ (h)
Rat ATII	23.3 ± 3.8	132 ± 13	5.9 ± 1.2	839 ± 178	11.5 ± 3.6
A459	8.9 ± 1.0	12.9 ± 0.9	4.3 ± 0.8	90 ± 15	8.9 ± 2.2

Experimental conditions and analyses were as described in the legend to Fig. 1 showing the time-course of accumulation of 0.3 μM ^{109}Cd in alveoar type II cells isolated from rats and in the A549 cells. The meaning of the parameters (A_0, $A_{e(f)}$, $A_{e(s)}$, $t_{1/2(f)}$ and $t_{1/2(s)}$) is given in the text. The values shown are the best-fit parameters ± SER values corresponding to Eq. (1).

Table 3
Tracer levels measured in A549 cells grown on petri dishes following exposure to 0.3 μM ^{109}Cd for different times with respect to different washing solutions

Time	Std (pmol/mg protein)	EDTA (pmol/mg protein)	EDTA-sensitive (%)
15 min	28 ± 6	26 ± 4	7.1
30 min	35 ± 7	36 ± 9	–
1 h	44 ± 11	41 ± 10	6.8
3 h	56 ± 9	53 ± 9	5.3
6 h	64 ± 13	66 ± 10	–
9 h	78 ± 18	75 ± 8	3.8
12 h	97 ± 19	100 ± 13	–

Following exposure for the desired time, cells were rapidly rinsed in the absence (Std) or in the presence (EDTA) of 2 mM EDTA added in the cold stop solution. Consequently, the relative percentage of EDTA-sensitive labile fraction of ^{109}Cd accumulation can has been calculated as explained in the text.

a 3-min and a 1-min period of exposure to 0.3 μM ^{109}Cd in the primary cultures (Fig. 2A) and the cell line (Fig. 2B), respectively. The data points obtained under various experimental conditions have been analyzed according to Eq. (2), and the parameter values are reported in Table 4. Data obtained using a standard stop solution (filled circles) reveal that ^{109}Cd is accumulated in the rat ATII cells about four times as fast as in the A549 cells ($v = 24.2 \pm 1.7$ vs. 5.7 ± 0.6 pmol/min/mg protein). Note, however, that the EDTA washing procedure (filled squares) leads to an apparent decrease of 26% in the initial rate of tracer accumulation in the rat ATII cells but not in the A549 cells, although no significant effect of EDTA rinses could be detected following longer exposure times (Table 2). Because the EDTA-sensitive component of tracer accumulation is believed to represent rapid adsorption and is not expected to increase with time, these results strongly suggest that a rapid efflux may occur during the washing step with EDTA in the rat ATII cells but not in the A549 cells.

Measurements performed in the presence of an excess of 300 μM unlabeled Cd (open circles), used as a specific inhibitor, reveal a specific (v_S, displaceable) and a nonspecific (v_{NS}, non displaceable) component of v. Only 10% and 14% of the total v is nonspecific in the primary cultures and the cell line, respectively. This nonspecific process of accumulation can easily be related to the diffusional component ($k_D[^{109}Cd]$). Now, if we assume that 300 μM unlabeled Cd completely inhibits the specific accumulation of 0.3 μM tracer, from the v_{NS} values of 2.5 ± 0.3 and 0.8 ± 0.2 pmol/mg obtained in the rat ATII and the A549 cells, k_D values of 8.3 ± 1 and 2.7 ± 0.7 pmol/min/μM/mg protein can be estimated for each cell sample, respectively. Thus, passive diffusion led to a threefold faster Cd accumulation in the rat ATII cells compared to the cell line. Note that in all cases of co-incubation with tracer and unlabeled Cd, data obtained following rinses with a standard or a 2 mM EDTA-containing stop solution were not significantly different (data not shown). Fig. 2 also shows the presence of a nonzero intercept value on the y axis, part of which is specific (A_{0S}), as revealed by its sensitivity to unlabeled Cd. From the parameter values reported in Table 4, it can be estimated that 70% and 49% of A_0 is specific for the rat ATII and the A549 cells, respectively. On the other hand, the part of A_0 that still remains in the presence of unlabeled Cd may represent rapid nonspecific adsorption and/or unwashed tracer, namely dead space (A_{0NS}). In accordance with this, EDTA-containing stop solution decreased but did not completely eliminate A_0 in both cell models. From the A_{0NS} values of 4.8 ± 0.4 and 2.3 ± 0.2 pmol/mg obtained for 0.3 μM tracer in the rat ATII and the A549 cells, K_d values of 16 ± 1.3 and 7.7 ± 0.7 pmol/μM/mg protein can be estimated for each cell sample, respectively. A twofold higher

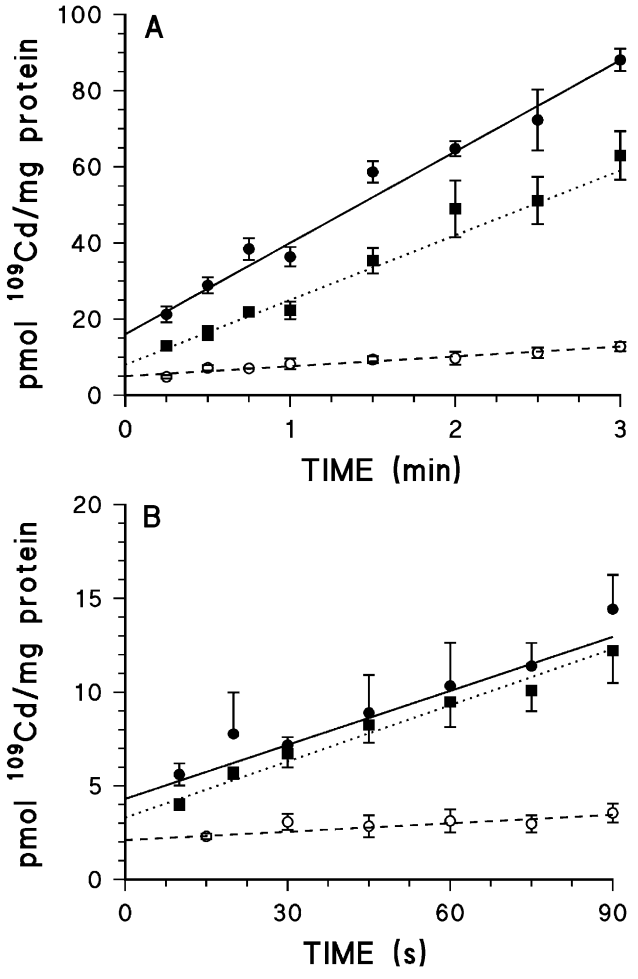

Fig. 2. Effect of an excess of unlabeled Cd (300 μM) in the transport medium or 2 mM EDTA in the stop solution on short-term cellular accumulation of 0.3 μM ^{109}Cd. Three-day-old rat ATII cells (A) and 14-day-old A549 cells (B) grown on petri dishes were exposed to tracer in the absence of unlabeled Cd and washed with standard (filled circles) or EDTA-containing (filled squares) stop solution or exposed to tracer in the presence of unlabeled Cd and washed with a standard stop solution (open circles). Values shown are the means ± S.D. evaluated in five determinations of the same subculture. The parameters obtained following linear regression analyses over the data points (Eq. (2)) are listed in Table 4.

nonspecific initial binding is observed in the rat type II cells. Now it appears that K_d and k_D should both be considered as part of the total nonspecific accumulation of tracer.

3.3. Kinetic parameters of Cd accumulation

The transport mechanism involved in Cd accumulation in each cell model was further characterized by determining the kinetic parameters by one-time point analysis, measuring the initial 1-min accumulation of 0.3 μM ^{109}Cd [T] in the presence of increasing concentrations of unlabeled Cd [S]. The data points obtained for the rat type II cells (Fig. 3A) and the A549 cells (Fig. 3B) could be well analyzed according to the modified Michaelis–Menten Eq. (6) with the following kinetic parameter values: for the ATII cells, $V_{max} = 873 \pm 109$ pmol/min/mg protein, $K_m = 6.4 \pm 1.3$ μM, $K_D = 23.6 \pm 1.8$ pmol/min/μM/mg protein; for the A549 cells, $V_{max} = 798 \pm 97$ pmol/min/mg protein, $K_m = 19.3 \pm 1.5$ μM, $K_D = 6.7 \pm 1.4$ pmol/min/μM/mg protein. Note that K_D values are in accordance with previous estimated values ($[K_d + k_D]$) in Fig. 2. A 3.5-fold higher proportionality constant K_D was determined for the nonspecific contributions to the total 1-min accumulation of Cd in the rat cells. Therefore, the part of K_D that represents passive diffusion (k_D) as well as the much higher specific uptake rate (v_S, Table 4) determined for Cd accumulation in the rat ATII cells may well account for the much higher levels of accumulation obtained in this cell model compared to the cell line.

3.4. Transepithelial transport of Cd

Because lung absorption involves Cd passage across the alveolar epithelium, the accumulation and transepithelial transport of 0.3 μM ^{109}Cd have also been studied in cell monolayers grown on filters, a culture system allowing access to the basolateral (BL) as well as to the apical (AP) side of the cells. Results of this study are shown in Fig. 4. In both cell models, the accumulation time-course of ^{109}Cd (filled circles) could be well analyzed according to Eq. (1) but different parameters were obtained compared to petri-dish culture conditions. Much lower levels of accumulation were recorded under filter-growth conditions for the rat ATII cells ($A_{e(f)} \sim 70$ vs. 130 pmol/mg protein; $A_{e(s)} \sim 600$ vs. 840 pmol/mg protein) but comparable $t_{1/2}$ values were estimated ($t_{1/2(f)} \sim 7$ vs. 6 min; $t_{1/2(s)} \sim 13$ vs. 11 h) (Fig. 4A). For ^{109}Cd accumulation in the A549 grown on filters (Fig. 4B), and contrary to what has been observed with cells grown on petri dishes, the fast process of accumulation, but not the slow one, was found responsible for most of the maximal cellular accumulation ($A_{e(f)} \sim 55$ vs. 13 pmol/mg protein; $A_{e(s)} \sim 35$ vs. 90 pmol/mg protein). Therefore, although $t_{1/2}$ values were similar whatever the culture conditions ($t_{1/2(f)} \sim 6$ vs. 4 min; $t_{1/2(s)} \sim 6$ vs. 9 h), the accumulation time-course of ^{109}Cd was clearly different in A549 cells grown on filters.

In both cell models, ^{109}Cd was highly transported across the cell monolayers (open triangles); an apparent P_{coeff} value of 67×10^{-7} and 46×10^{-7} cm/s could be estimated for the rat and the A549 cells, respectively (average cell density of 0.3 and 0.8 mg/filter for the primary culture and the cell line, respectively). Interestingly, the accumulation and transport time-courses were found parallel in ATII cell monolayers; a constant ratio of cellular-to-basolateral ^{109}Cd level (decreasing only from 1.8 to 1.3 between 1 and 12 h of exposure) was measured during the period of time studied. In contrast, transport across the A549 cells increased significantly after the cellular accumulation had plateaued; the ratio of cellular-to-basolateral tracer level decreased dramatically from 2.2 to 0.7 during the 12-h period studied.

Now, considering an average cell density of 0.3 mg/filter for the rat ATII cells, cellular Cd accumulation of about 402 pmol/mg protein recorded following a 12-h exposure to 0.3 μM ^{109}Cd can be converted to ~ 121 pmol/filter. Similarly,

Table 4
Specific, nonspecific and EDTA-sensitive zero-time intercept A_0 and initial rate v of accumulation

Conditions	Zero-time intercept (pmol/mg protein)			Initial rates (pmol/min/mg protein)		
	A_0	A_{0S}	A_{EDTA}	v	v_S	v_{EDTA}
Rat ATII						
Ctrl	16.1 ± 1.6	11.3 ± 2.0	8.3 ± 2.6	24.2 ± 1.7	21.7 ± 2.0	6.4 ± 2.0
EDTA	7.8 ± 1.0	–	–	17.8 ± 1.1	–	–
Cd	48 ± 0.4	–	–	2.5 ± 0.3	–	–
A549						
Ctrl	4.5 ± 0.4	2.2 ± 0.6	1.2 ± 0.7	5.7 ± 0.6	4.9 ± 0.8	NIL
EDTA	3.3 ± 0.3	–	–	6.0 ± 0.4	–	–
Cd	2.3 ± 0.2	–	–	0.8 ± 0.2	–	–

Experimental conditions and analyses were as described in the legend to Fig. 2. Values shown are the best-fit parameters ± SER obtained by linear regression analyses of the data recorded for the rat type II alveolar cells (Fig. 2A) and the A549 cells (Fig. 2B). The parameters A_0 and v represent the intercept and the slope of the regression lines, respectively. Specific A_{0S} and v_S fractions were calculated by subtraction of the total values obtained in the presence of 300 μM unlabeled Cd (Cd) from the total values estimated under control conditions (Ctrl, 0.3 μM ^{109}Cd alone). EDTA-sensitive fractions A_{EDTA} and v_{EDTA} were calculated by subtraction of values measured following washing procedure using 2 mM EDTA from the respective values measured with standard ^{109}Cd-free stop solution.

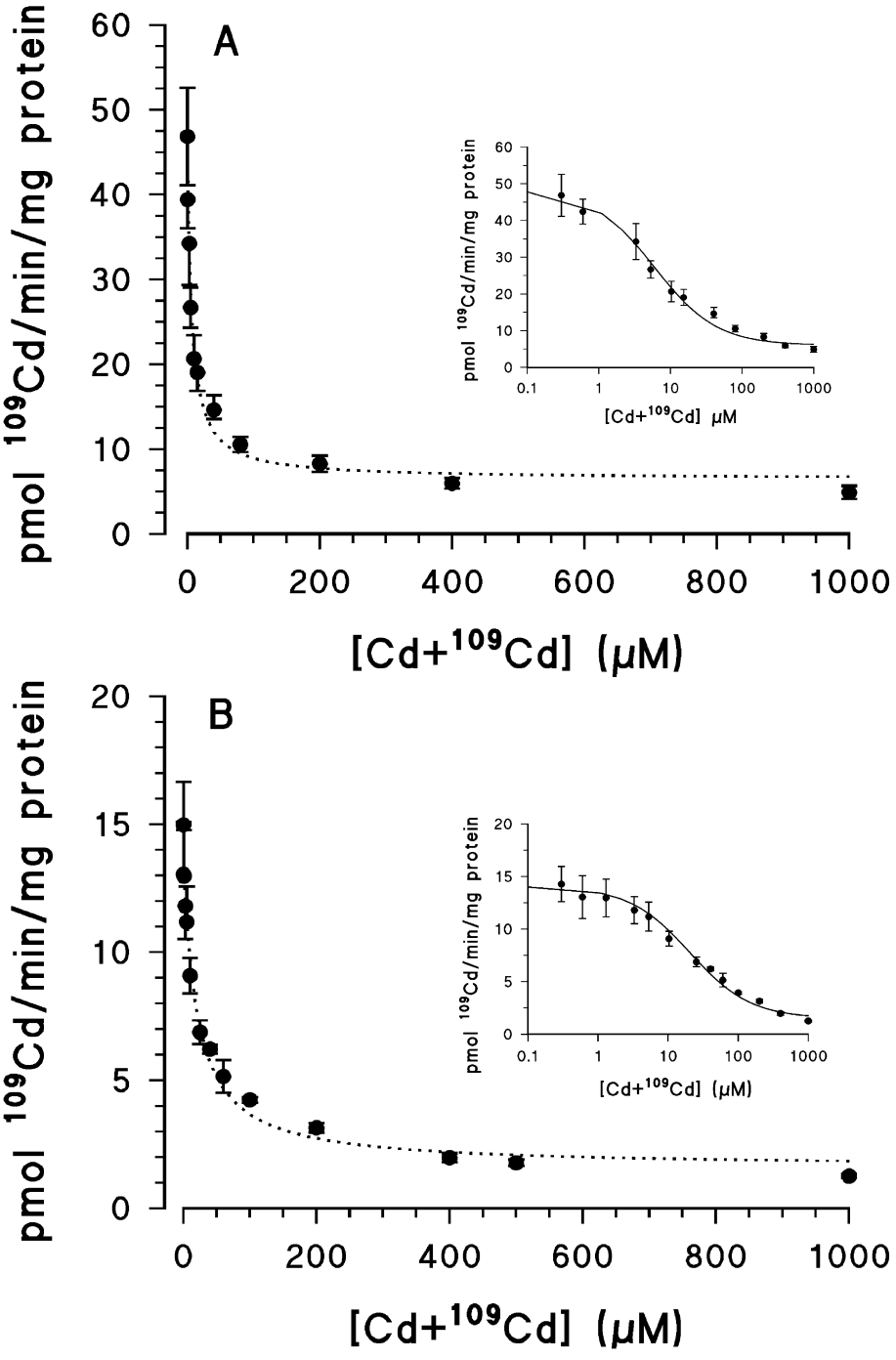

Fig. 3. Determination of kinetic parameters for ^{109}Cd influx in 3-day-old rat ATII cells (A) and 14-day-old A549 cells (B) grown on petri dishes. Initial accumulation values were estimated by one-time point analysis (1 min) as described in the text using a tracer ^{109}Cd concentration of 0.3 μM and unlabeled Cd concentrations ranging from 0 to 1000 μM. Values shown are the means ± S.D. evaluated in five determinations of the same subculture. The lines shown are the best-fit curves to Eq. (6) with the following kinetic parameter values: (A) $K_m = 6.4 \pm 1.3$ μM, $V_{max} = 873 \pm 109$ pmol/min/mg protein, $K_D = 23.6 \pm 1.8$ pmol/min/μM/mg protein; (B) $K_m = 19.3 \pm 1.5$ μM, $V_{max} = 798 \pm 97$ pmol/min/mg protein, $K_D = 6.7 \pm 1.4$ pmol/min/μM/mg protein. Insets: the log scale on the *x* axis allows a better presentation of the kinetic data.

the AP-to-BL transport value of 308 pmol/mg protein can be converted to 92 pmol/filter. Thus, 213 pmol (121 + 92 pmol) of tracer would be lost from the AP medium within 12 h. Considering an initial amount of 600 pmol (2 ml of 0.3 μM), AP Cd concentration fell to 0.194 μM (600−213 pmol/2 ml) after 12 h. Similarly, and considering an average cell density of 0.8 mg/filter for the A549 cells, the residual AP level of ^{109}Cd can be estimated to 0.198 μM (600−204 pmol/2 ml) after 12 h. These estimates agree with direct measurements of Cd level in the AP medium following a 12-h exposure

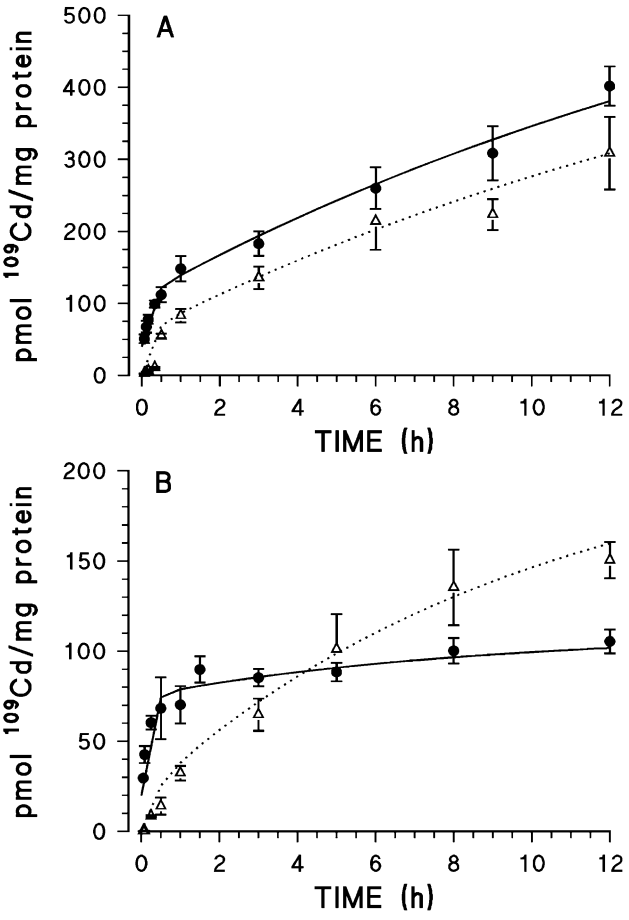

Fig. 4. Time-course of 0.3 μM ^{109}Cd cellular accumulation and transepithelial transport in 3-day-old rat ATII cells (A) and 14-day-old A549 cells (B) grown on filters. Cells were exposed to tracer on the apical side and cellular level (filled circles), and total amounts of tracer recovered in the basolateral chamber of the inserts (open triangles) were measured as explained in the text. Values shown are the means ± S.D. evaluated in three determinations of different cultures. The lines shown are the best-fit curves through data points, as obtained according to Eq. (1).

(0.178 and 0.187 μM for the rat ATII and the A549 cells, respectively).

3.5. Kinetics of Cd efflux

The transepithelial transport of Cd may be the result of important transcellular (cellular metal release in the BL medium) and/or paracellular pathways (leakage through tight junctions). To estimate the relative contribution of the transcellular pathways in the transepithelial transport of Cd, the time-course of cellular ^{109}Cd efflux was studied following a 1-h preincubation at 0.3 μM ^{109}Cd on the apical (AP) side (Fig. 5). For both cell models, cellular tracer efflux data (filled circles) could be well analyzed according to the first-order decay Eq. (3). Parameter values reported in Table 5 reveal a rapid process of efflux in both cell models (parameters $t_{1/2E}$) but most of the ^{109}Cd remained in the cells, especially for the A549 cells (parameters E_e relative to E_0). Indeed, the estimated relative amounts of ^{109}Cd lost ($[E_0 - E_e]/E_e \times 100$) are 52% and 35% for the rat ATII and the A549 cells, respectively. These results, together with the data reported in Table 2, reveal that Cd efflux cannot be exclusively attributed to metal desorption from the cell surface.

In parallel to the measurements of cellular ^{109}Cd contents, the amount of tracer recovered in either the AP or the BL medium was also recorded during the efflux studies. Data obtained could be well analyzed according to the first order rate Eq. (4). The parameter values reported in Table 6 reveal that tracer is significantly recovered in the AP (filled triangles) as well as in the BL (open triangles) compartment. However, tracer levels in AP medium were twice that in the BL medium for both cell models; two thirds of the total

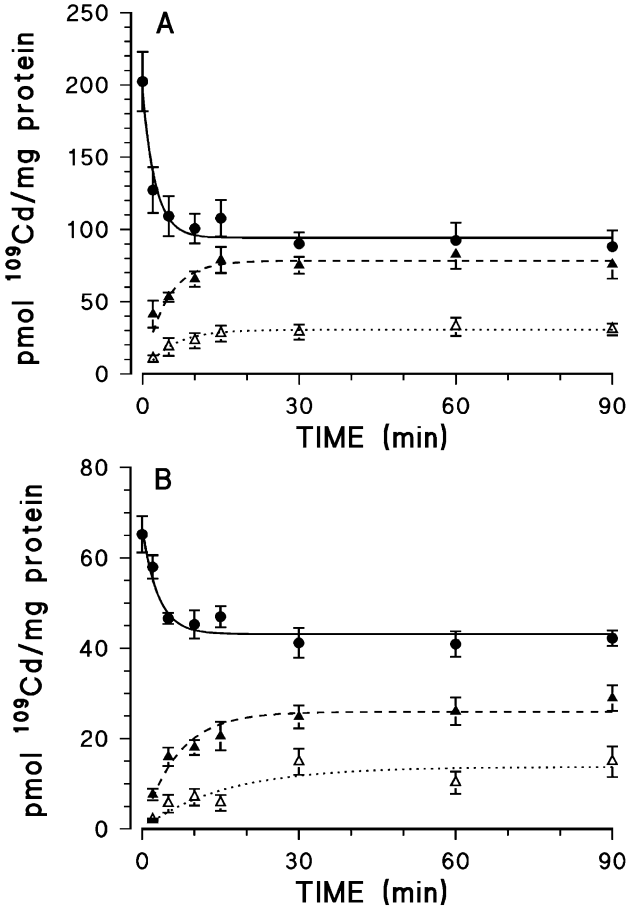

Fig. 5. Kinetics of ^{109}Cd efflux from 3-day-old rat ATII cells (A) and 14-day-old A549 cells (B) grown on filters and preexposed to 0.3 μM ^{109}Cd on the apical side for 1 h. Cellular ^{109}Cd release (filled circles) and the concomitant appearance of tracer in the apical (filled triangles) and the basolateral (open triangles) medium were recorded as described in the text. Lines show the best fit-curves through the data points (the means ± S.D. evaluated on three different cell cultures) corresponding to the first-order decay Eq. (3) (cellular release) and to the first-order rate Eq. (4) (tracer appearance in the efflux media). The efflux parameters are listed in Tables 5 and 6.

Table 5
Efflux parameters describing the time-course of cellular ^{109}Cd release

	E_0 (pmol/mg protein)	E_e (pmol/mg protein)	$t_{1/2E}$ (min)
Rat ATII	201 ± 10	96.4 ± 3.5	1.3 ± 0.3
A549	65.5 ± 2.3	42.5 ± 1.2	3.1 ± 0.8

Experimental conditions and analyses were as described in the legend to Fig. 4 showing the efflux time-course of ^{109}Cd following a 1-h preincubation with 0.3 μM ^{109}Cd. The meaning of the parameters E_0, E_e and $t_{1/2E}$ is given in the text. Values shown are the best-fit parameters ± SER obtained by regression analyses of the data recorded for the rat type II alveolar cells and the A549 cells according to Eq. (3).

^{109}Cd lost from the cell was recovered in the AP compartment. Also, the appearance of tracer in the BL medium occurred much more slowly than Cd release from the AP side of the cell monolayers (compare parameter $t_{1/2R}$ values for AP and BL recovery in Table 6).

3.6. Monolayers permeability properties

Efflux studies strongly suggest that transcellular pathways, although being significant, are not mainly responsible for the high level of ^{109}Cd transported across cell monolayers. The paracellular pathways were thus investigated by measuring monolayers permeability to ^{3}H-mannitol. The transport time-course of 0.3 μM ^{3}H-mannitol from the AP to the BL medium (Fig. 6A) clearly shows that the A549 cell monolayers (filled circles) are much more "leaky" than the primary cultures (open circles). Indeed, from initial (30 min) transport measurements, an apparent P_{coeff} value of 3×10^{-7} and 29×10^{-7} cm/s can be estimated for the ATII and the A549 cell monolayers, respectively. Moreover, nonlinear regression analysis of the data point according to Eq. (4) (where R is changed to T: transport, and $t_{1/2R}$ to $t_{1/2T}$) reveal a sevenfold higher equilibrium transport value for the cell line compared to the primary cultures (118 ± 11 vs. 16 ± 1 pmol/mg protein). Note that the ^{3}H-mannitol content in cell monolayers remained negligible in both cell samples (Fig. 6B); clearly, dead space does not contribute appreciably to the cellular ^{109}Cd accumulation estimated previously (Figs. 1 and 4).

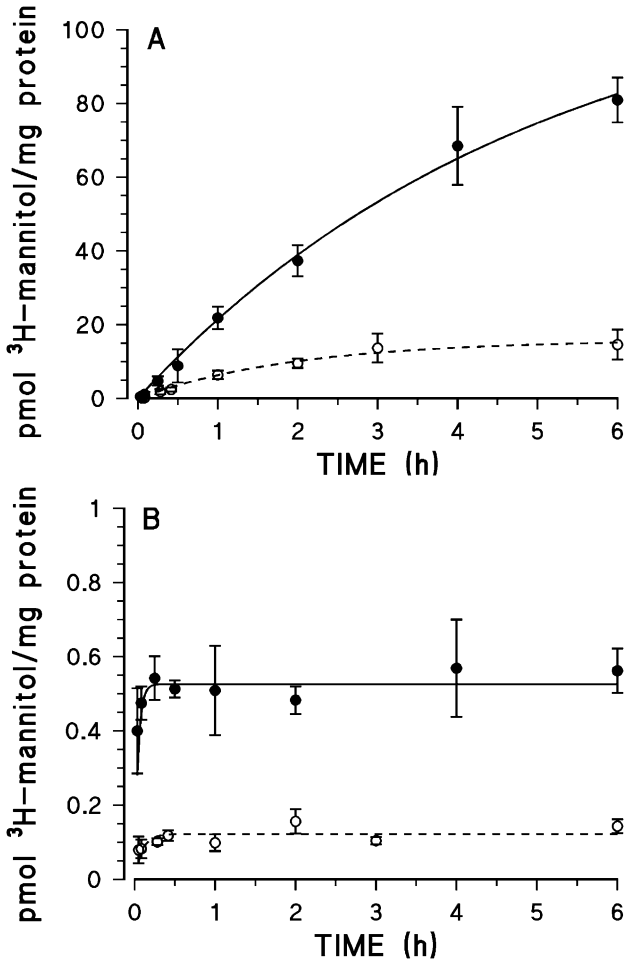

Fig. 6. Time-course of 0.3 μM ^{3}H-mannitol transepithelial transport (A) and monolayer accumulation (B) in 3-day-old rat ATII cells (open circles) and 14-day-old A549 cells (filled circles) grown on filters. Cells were exposed to tracer on the apical side, and the cellular level as well as total amounts of tracer recovered in the basolateral chamber of the inserts were measured as explained in the text. Values shown are the means ± S.D. evaluated in five determinations of the same subcultures. The lines shown are the best-fit curves through data points, as obtained according to Eq. (4).

Table 6
Parameters describing the time-course of ^{109}Cd appearance in the AP and BL compartments during the cellular tracer release

	R_e (pmol/mg protein)	$t_{1/2R}$ (min)
Rat ATII		
AP	76.8 ± 3.0	2.5 ± 0.4
BL	30.4 ± 1.0	4.1 ± 0.5
A549		
AP	26.2 ± 1.3	5.2 ± 0.9
BL	13.3 ± 1.8	11.6 ± 3.7

Experimental conditions and analyses were as described in the legend to Fig. 4 showing the efflux time-course of ^{109}Cd following a 1-h preincubation with 0.3 μM ^{109}Cd. The meaning of the parameters R_e, and $t_{1/2R}$ is given in the text. Values shown are the best-fit parameters ± SER obtained by regression analyses of the data recorded for the rat type II alveolar cells and the A549 cells according to Eq. (4).

4. Discussion

4.1. Higher levels of Cd accumulation as well as initial uptake rate in the rat ATII cells

The pulmonary toxicity of Cd has been largely studied using primary cultures of rat ATII cells as well as the human cell line A549. However, very few investigations have been devoted to the mechanisms of Cd transport into alveolar cells. Here we show that Cd accumulation in both cell models involves a three-step mechanism. Indeed, data

obtained over a 12-h exposure were analyzed according to Eq. (1) describing: (1) a zero-time accumulation that shows up as a nonzero intercept (A_0 in Figs. 1 and 2); (2) a fast process of accumulation A_f, which proceeds within minutes; (3) a much slower process A_s, which takes hours (Table 1). Each of these steps gives much higher levels of uptake in the rat ATII cells compared to the A549 cell line. The EDTA-sensitive labile fraction of accumulation was found negligible in both cell models: Cd accumulates into the alveolar cells and the much higher uptake levels measured in the primary cultures cannot be related to higher level of adsorption onto the external surface of the cell membrane (Tables 2 and 3). Our results also show that, although no significant differences could be observed between the $t_{1/2}$ values of each process of accumulation (Table 1), Cd is taken up much more rapidly in the rats ATII (Fig. 2). This more rapid accumulation could be related to higher initial uptake rate for specific (v_S) as well as for nonspecific (v_{NS} or k_D) transport of Cd in the primary cultures (Table 4).

The Cd accumulation time-course has been studied in the T27 clone of the A549 cells; no equilibration in cellular Cd level could be observed for up to 8 h exposure to 5 μM ^{109}Cd, although accumulation values of 0.5 μmol/10^9 cells were measured [19]. Considering an average cell content of 2.3×10^6 cells/dish and an average cell density of 0.9 mg/dish in our studies, the uptake value of ~ 67 pmol/mg protein obtained following an 8-h exposure to 0.3 μM ^{109}Cd can be converted to ~ 26 pmol/10^6 cells or 0.026 μmol/10^9 cells. Interestingly, a comparison with uptake values obtained by Kang et al. [19] reveals a direct correlation between cellular Cd accumulation and the exposure concentration (0.5 and 0.026 μmol/10^9 cells following an 8-h exposure to 5 and 0.3 μM ^{109}Cd, respectively) although differences in Cd uptake levels have been reported between subpopulations of A549 cells [27]. Note that, in accordance with previous studies showing no significant cytotoxicity in a rat cell line that resembles ATII cells following an 8-h exposure to 50 μM Cd or less [20], cell viability was not affected by 0.3 μM Cd up to 12 h (data not shown). Also, our experimental conditions are not expected to modify cellular thiol levels nor to induce any stress proteins since exposure to 5 μM $CdCl_2$ up to 8 h did not succeed in reducing GSH content [28] nor in stimulating HSP 72 synthesis in the A549 cells [29].

4.2. Specific system of higher affinity for CD in the rat ATII cells

Specific systems of transport of similar capacity but different affinities (threefold higher for the rat ATII cells) were characterized for Cd accumulation in the two cell models: for the ATII cells, $V_{max} = 873 \pm 109$ pmol/min/mg protein, $K_m = 6.4 \pm 1.3$ μM; $K_D = 23.6 \pm 1.8$ pmol/min/μM/mg protein; for the A549 cells, $V_{max} = 798 \pm 97$ pmol/min/mg protein, $K_m = 19.3 \pm 1.5$ μM, $K_D = 6.7 \pm 1.4$ pmol/min/μM/mg protein. The K_m values predict 98% and 96% inhibition of the specific 1-min accumulation of 0.3 μM ^{109}Cd by 300 μM unlabeled Cd in the rat ATII and the A549 cells, respectively, in agreement with the results reported in Table 4. Saturation for ^{109}Cd transport in the A549 cells has also been observed by Kang et al. [19]; a half-maximal accumulation was noted for ~ 2.5 μM with no evidence for any nonspecific component. However, direct comparison with our results is difficult since these authors have considered the 8-h accumulation values. As explained earlier, they did not observe any equilibration in Cd accumulation during this time of exposure, whereas in our studies, initial uptake rate conditions, namely linearity of the uptake-time course, are only 2 min. Future studies testing, for example, inhibition by other metals and/or well known inhibitors specific to transport systems, should give insights into the transport mechanisms responsible for Cd uptake/efflux in alveolar lung cells. It should be noted that although kinetic data did not reveal any heterogeneity, more than one of the Cd species present in the exposure medium (Cd^{2+}, $CdCl_n^{2-n}$) may conceivably participate in the transport process [30].

Now, considering that the specific uptake at $t = 0$ (A_{0S}), as well as the true specific initial uptake rate (v_S) both contribute to the 1-min accumulation (A_1), the following equality then holds (Eq. (8))

$$A_1 = A_{0S} + v_{S1} \tag{8}$$

in which v_{S1} is equivalent to v_S normalized to 1-min uptake. Because data analysis failed to detect the presence of more than one Michaelis–Menten component, the respective contribution of A_{0S} and v_{S1} to A_1 measured at any ^{109}Cd concentration should be directly proportional to their maximum values. Since the data reported in Table 4 show that A_{0S} and v_{S1} account, respectively, for 34% and 66% of the total 1-min uptake, a $A_{(0)max}$ of ~ 297 pmol/mg protein and a $V_{(1)max}$ value of ~ 576 pmol/mg protein can be estimated for Cd accumulation in the rat ATII cells. Similarly, a $A_{(0)max}$ of ~ 247 pmol/mg protein and a $V_{(1)max}$ value of ~ 551 pmol/mg protein can be estimated for the cell line.

4.3. Significant contribution of paracellular pathways to the transepithelial transport of Cd

The time-course of accumulation and transport of ^{109}Cd through cell monolayers grown on filters revealed a significant transepithelial transport in both cells models. These results contrast with our previous data obtained in Caco-2 cells under similar conditions showing that transepithelial transport of Cd in this human intestinal cell line never exceeds 3% of the cellular accumulation [26]. High P_{coeff} values ($46–67 \times 10^{-7}$ cm/s) have been determined for Cd permeability in rat ATII and A549 cell monolayers, a result in accordance with the reported high bioavailability of the inhaled metal in animal models [31,32]. Some studies have revealed that Cd may rapidly disrupt the paracellular barrier without causing a significant loss of

viability: (i) exposure to 20–60 μM Cd decreased the TEER value in the LLC-PK1 kidney cells [33]; (ii) a 4-h exposure to Cd concentrations higher than 25 μM increased the P_{coeff} to mannitol and PEG-4000 and significantly reduced the TEER values in the Caco-2 intestinal cells [34]. Accordingly, the fact that 0.3 μM Cd (Figs. 1 and 4) may affect the permeability of rat ATII or A549 cell monolayers exposed for 12 h cannot be excluded. Although much less probable because of the very short exposure time, Cd up to 1000 μM may conceivably modify the paracellular barrier, thus increasing its own transport. However, Cd accumulation data as well as the kinetic parameter values are not expected to be much affected in the case of the disruption of junction proteins since most of our results strongly suggest that dead space (including intercellular space) does not contribute appreciably to the cellular accumulation estimation.

Now, considering an initial amount of 600 pmol in the AP medium and the AP-to-BL transport values of 92 and 120 pmol/filter measured after 12 h for the ATII and the A549 cells, respectively, it appears that 15% and 20% of the metal is transported across the cell monolayers after 12 h. However, it clearly appears that the Cd concentration in the BL medium remains much lower compared the AP level. Indeed, considering that 92 pmol (for ATII cells) and 120 pmol (for A549 cells) were recovered in a total BL volume of 3 ml, tracer BL concentrations of 0.030 and 0.049 μM can thus be estimated. Comparison with the estimated residual concentration of Cd in the AP medium (0.194 and 0.198 μM for the ATII and the A549 cells, respectively) clearly reveals no equilibration for Cd between the two compartments, which argues against the possibility of a complete paracellular barrier disruption under our experimental conditions. Interestingly, a 12-h exposure resulted in similar Cd depletion from the AP medium in the two cell models but the respective contribution of the cellular accumulation and the transepithelial transport varied with respect to the cell samples: in the rat ATII cells, 57% and 43% of tracer depletion was related to the cellular accumulation and the transport across cell monolayers, respectively, whereas these contributions were estimated to be 41% and 59%, respectively, in the A549 cells.

Efflux studies performed following preloading of cells for 1 h at the apical side revealed that only half and one third of the accumulated metal is released out of the ATII and the A549 cells, respectively. A higher percentage of Cd retention is expected for a pre-exposure time sufficiently long to induce synthesis of cysteine-rich proteins, thus increasing the overall cell capacity to bind Cd. Indeed, studies have reported that a 12-h and an 8-h exposure to 10 μM Cd significantly increased the MT mRNA and protein level in A549 and rat ATII cells, respectively [19,20]. Interestingly, some of these studies also reported no significant change in Cd accumulation after cell treatment with BSO (DL-buthionine-sulfoximine) or DEM (diethyl maleate) used to modify cellular GSH and MT levels, suggesting that these peptides would not necessarily represent the major binding sites for intracellular Cd.

About one third of the metal lost is recovered in the basolateral medium. These results contrast with our previous data obtained in Caco-2 cells showing that metal efflux in the basolateral medium following cell preexposure on the apical side remained negligible [26]. Contribution of transcellular pathways to the transepithelial transport of Cd is much more important for alveolar cell monolayers compared to intestinal cell monolayers. However, these pathways are not mainly responsible for the high level of ^{109}Cd transported across cell monolayers. Unfortunately, we were not able to detect any significant transepithelial electrical resistance (TEER) across rat ATII or A459 cell monolayers, an observation that has also been reported by others [14]. Numerous studies have shown that the A549 cells express various junctional (including ZO-1, JAM and E-cadherin) and basement membrane proteins [35–37]. In spite of these features, very few investigators have been able to measure a significant TEER value for confluent A549 cell monolayers [38,39], whereas TEER values up to 2000 Ω cm^2 have been reported for primary cultures of ATII cells [40]. It has been suggested that ATI and ATII cells in vivo may form tighter monolayers than in vitro system. Here, we found that, P_{coeff} for mannitol was higher in the A549 cell monolayers compared to the primary cultures (29 vs. 3×10^{-7} cm/s) although similar values were obtained for ^{109}Cd permeability in both cell models. However, these results agree with data showing a higher transepithelial transport of ^{109}Cd (Fig. 4) but a lower cellular tracer efflux in the cell line (Fig. 5). The contribution of the paracellular pathways to the transepithelial transport of Cd would be higher for the A549 cells, whereas that of the transcellular pathways would be more important for the rat ATII cells. Interestingly, maximal transport value estimated for the A549 cells does not predict any equilibration for ^{3}H-mannitol between the two compartments (AP and BL). These results suggest that A549 cell monolayers are not fully leaky, an observation that supports other data showing that A549 cells do form barriers relatively resistant to Lucifer yellow [14]. However, the A549 cell monolayers would not be as tight as the primary cultures: an apparent BL-to-AP ratio of 1:10 but only 1.6:300 could be estimated for the ^{3}H-mannitol concentration at equilibrium for the A549 and the ATII cell monolayers, respectively.

5. Conclusions

We have shown that high levels of Cd accumulate in the ATII phenotype but Cd transport was much more rapid and led to higher levels of accumulation in the primary cultures of rat ATII cells compared to the human A549 cell line. These differences could not be attributed to a higher level of adsorption onto the external surface of the cell membrane in the rat ATII cells. In both cell models, a specific system of transport could be characterized with a threefold higher

affinity for Cd in the rat ATII cells. Cadmium influx was found to be only partially reversible, with about half and one third of the accumulated metal remaining in the rat ATII and the A549 cells, respectively, most probably tightly bound to intracellular compounds. Although confluent cell monolayers were found not to be fully leaky for both cell models, A549 cell monolayers showed greater permeability to mannitol; accordingly a significant transepithelial transport was observed for Cd in this cell model. Also, we have demonstrated that although two lung cell models may have similar P_{coeff} values for Cd, different contributions of the para- and transcellular pathways may be significant. These differences in transport properties may modify the dose–response curve for Cd toxicity, the limit of extrapolation taken into account when evaluating metal transport and/or toxicity using these two cell models.

Acknowledgements

This research was supported by the Natural Sciences and Engineering Research Council of Canada, NSERC (Jumarie, grant RGPIN-203202098). The author thanks Daniel Goulet the technical assistance.

References

[1] P.A. Tibbits, W.C. Milroy, Mil. Med. 145 (1980) 435–437.
[2] R.B. Hayes, Cancer Causes Control 8 (1997) 371–385.
[3] C.J. Lin, P.C. Yang, M.T. Hsu, F.H. Yew, T.Y. Liu, C.T. Shun, S.W. Zyan, T.C. Lee, Toxicology 127 (1998) 157–166.
[4] C.R. Timblin, Y.M. Janssen, J.L. Goldberg, B.T. Mossman, Free Radic. Biol. Med. 24 (1998) 632–642.
[5] J. Heyder, Eur. J. Respir. Dis. 63 (1982) 29–50.
[6] U. Glaser, H. Klöppel, D. Hochrainer, Ecotoxicol. Environ. Saf. 11 (1986) 261–271.
[7] Z.P. Feng, R.B. Clark, Y. Berthiaume, Am. J. Respir. Cell Mol. Biol. 9 (1993) 248–254.
[8] G. Yue, S. Matalon, Am. J. Physiol. 272 (1997) L407–L412.
[9] J.P. Gotze, P. Lindeskog, C.S. Tornquist, Environ. Health Perspect. 102 (1994) 147–156.
[10] Y. Kikkawa, F. Smith, Lab. Invest. 49 (1983) 122–139.
[11] J.S. Lwebuga-Mukasa, Am. Rev. Respir. Dis. 144 (1991) 452–457.
[12] M. Lieber, B. Smith, A. Szakal, A. Nelson-Rees, G. Todaro, Int. J. Cancer 17 (1976) 62–70.
[13] B.T. Smith, Am. Rev. Respir. Dis. 115 (1977) 285–293.
[14] K.A. Foster, C.G. Oster, M.M. Mayer, M.L. Avery, K.L. Audus, Exp. Cell Res. 243 (1998) 359–366.
[15] H. Mairbäurl, R. Wodopia, S. Eckes, Am. J. Physiol. 273 (1997) L797–L806.
[16] A. Lazrak, A. Smanta, S. Matalon, Am. J. Physiol. 278 (2000) L848–L857.
[17] A. Kleinzeller, C. Dodia, A. Chander, A.B. Fisher, Am. J. Physiol. 267 (1994) C1279–C1287.
[18] M.D. Enger, J.G. Tesmer, G.L. Travis, S.S. Barham, Am. J. Physiol. 250 (1986) C256–C263.
[19] Y.-J. Kang, J.A. Clapper, M.D. Enger, Cell Biol. Toxicol. 5 (1989) 249–259.
[20] Q. Gong, B.A. Hart, Toxicology 119 (1997) 179–191.
[21] L.G. Dobbs, R. Gonzalez, M.C. Williams, Am. Rev. Respir. Dis. 134 (1986) 141–145.
[22] S.L. Sigurdson, J.S. Lwebuga-Mukasa, Exp. Cell Res. 213 (1994) 71–79.
[23] Z. Borok, A. Hami, S.I. Danto, S.M. Zabski, E.D. Crandall, Am. J. Respir. Cell Mol. Biol. 12 (1995) 50–55.
[24] L. Campbell, A.J. Hollins, A. Al-Eid, G.R. Newman, C. von Ruthland , M. Gumbleton, Biochem. Biophys. Res. Commun. 262 (1999) 744–751.
[25] C. Jumarie, P.G.C. Campbell, A. Berteloot, M. Houde, F. Denizeau, J. Membr. Biol. 158 (1997) 31–48.
[26] C. Jumarie, P.G.C. Campbell, M. Houde, F. Denizeau, J. Cell. Physiol. 180 (1999) 285–297.
[27] Y.-J. Kang, S.T. Nuutero, J.A. Claper, P. Jenkins, M.D. Enger, Toxicology 61 (1990) 195–203.
[28] Y.-J. Kang, M.D. Enger, Toxicology 48 (1988) 93–101.
[29] Y. Gaubin, F. Vaissade, F. Croute, B. Beau, J.-P. Soleilhavop, J.-C. Murat, Biochim. Biophys. Acta 1495 (2000) 4–13.
[30] C. Jumarie, C. Fortin, M. Houde, P.G.C. Campbell, F. Denizeau, Toxicol. Appl. Pharmacol. 170 (2001) 29–38.
[31] U. Glaser, H. Kloppel, D. Hochrainer, Ecotoxicol. Environ. Saf. 11 (1986) 261–271.
[32] H.J. Klimisch, Toxicology 84 (1993) 103–124.
[33] W.C. Prozialeck, R.J. Niewenhuis, Toxicol. Appl. Pharmacol. 107 (1991) 81–97.
[34] E. Duizer, A.J. Gilde, C.H.M. Versantvoort, J.P. Groten, Toxicol. Appl. Pharmacol. 155 (1999) 117–126.
[35] H.L. Winton, H. Wan, M.B. Cannell, D.C. Gruenert, P.J. Thompson, D.R. Garrod, G.A. Stewart, C. Robinson, Clin. Exp. Allergy 28 (1998) 1273–1285.
[36] Y. Liu, A. Nusrat, F.J. Schnell, T.A. Reaves, S. Walsh, M. Pochet, C.A. Parkos, J. Cell. Sci. 113 (2000) 2363–2374.
[37] J.C. Lacherade, A. Van de Louw, E. Planus, E. Escudier, M.P. D'Ortho , C. Lafuma, A. Harf, C. Delclaux, Am. J. Physiol., Lung Cell. Mol. Physiol. 281 (2001) L134–L143.
[38] S. Kobayashi, S. Kondo, K. Juni, Pharm. Res. 12 (1995) 1115–1119.
[39] E.J. Carolan, T.B. Casale, Am. J. Respir. Cell Mol. Biol. 15 (1996) 224–231.
[40] H. Yamahara, C.M. Lehr, V.H.L. Lee, K.J. Kim, Eur. J. Pharm. Biopharm. 40 (1994) 294–298.